Polymer 55 (2014) 235–247

Contents lists available at ScienceDirect

Polymer

journal homepage: www.elsevier.com/locate/polymer

Thermal analysis of disulfonated poly(arylene ether sulfone) plasticized with poly(ethylene glycol) for membrane formation

Hee Jeung Oh [a], Benny D. Freeman [a], James E. McGrath [b], Chang Hyun Lee [c], Donald R. Paul [a,*]

[a] The University of Texas at Austin, Department of Chemical Engineering, Austin, TX 78712, USA
[b] Virginia Polytechnic Institute and State University, Department of Chemistry, Blacksburg, VA 24061, USA
[c] Dankook University, Department of Energy Engineering, Cheonan, South Korea

ARTICLE INFO

Article history:
Received 17 October 2013
Received in revised form
23 November 2013
Accepted 26 November 2013
Available online 5 December 2013

Keywords:
Sulfonated polysulfone
Poly(ethylene glycol)
Melt processing

ABSTRACT

One route to melt processing of high glass transition temperature polyelectrolytes, such as disulfonated poly(arylene ether sulfone) (BPS), involves mixing a plasticizer with the polymer. In this study, poly(ethylene glycol) (PEG) was used as a plasticizer for BPS. BPS and PEG are miscible, and the effect of PEG molecular weight (in the range of 200–600 g/mol) and concentration on the T_g of BPS/PEG blends was investigated. As PEG molecular weight decreases and concentration increases, the blend T_g is depressed significantly. Based on isothermal holds in a rheometer at various temperatures and times, the PEG materials considered were thermally stable up to 220 °C for 10 min in air or 250 °C for at least 10 min under a nitrogen atmosphere, which is long enough to permit melt extrusion of such materials.

1. Introduction

Reverse osmosis (RO) is a dominant technology for desalinating water [1,2]. Currently, polyamide (PA) thin film composite membranes are widely used in RO because of their good transport properties and stability over a wide range of pH [3,4]. However, these PA membranes have poor resistance to aqueous chlorine, which is often added as a disinfectant to prevent membrane fouling, so feed water must be de-chlorinated before contacting the membrane to avoid serious membrane degradation [1,3,5]. This additional step increases operation costs. Additionally, desalination membranes are produced via solution processing methods [6]. For example, the PA thin film composite membranes mentioned above are made by interfacial polymerization of monomers at an oil/water interface [4,6]. Large volumes of volatile, flammable hydrocarbon solvents are used in this process.

Sulfonated polysulfones have been of interest for desalination because of their good chlorine resistance over a broad pH range, potentially making the de-chlorination step in desalination processes unnecessary [3,5,7,8]. Such membranes can be formed by typical solvent casting processes [3,5,8]. However, with appropriate plasticizers, sulfonated polysulfone membranes might be prepared by a melt extrusion process, avoiding the use of organic solvents in processing. Interestingly, sulfonated polysulfone can be plasticized using low molecular weight, water soluble poly(ethylene glycol) (PEG) [9,10]. This plasticizer can potentially be removed from the membrane by water extraction following melt processing. Furthermore, composite membranes could be formed by laminating the sulfonated polysulfone layer to a porous support or even using a coextrusion step wherein the support layer could be rendered porous by some means such as stretching [11]. Moreover, extruded membranes may have interesting properties compared to those of solution cast membranes, since morphology and transport properties of such materials are known to be sensitive to thermal processing history [7,12].

Bebin et al. proposed extruding post-polymerization sulfonated polysulfone (sPSU) films for proton exchange membrane fuel cells (PEMFCs) and compared proton conductivity and life span of extruded films to those of solvent cast films [13,14]. Sanchez et al. studied the effect of various plasticizers on the glass transition temperature and rheological behavior of post-polymerization sulfonated polysulfone to optimize extrusion conditions for PEMFCs [15–19].

In this study, we report results of studies whose long-term objective is to prepare melt extrudable formulations of disulfonated poly(arylene ether sulfone)s with PEG plasticizers. This paper

* Corresponding author. The University of Texas at Austin, Department of Chemical Engineering, 1 University Station, Mail Code: C0400, Austin, TX 78712, USA. Tel.: +1 512 471 5392; fax: +1 512 471 0542.
E-mail address: drp@che.utexas.edu (D.R. Paul).

0032-3861/$ – see front matter © 2013 Elsevier Ltd. All rights reserved.
http://dx.doi.org/10.1016/j.polymer.2013.11.041

summarizes the miscibility of PEG with the sulfonated polysulfone, the influence of PEG molecular weight and concentration in the blend on the glass transition temperature, and the thermal stability of PEGs at temperatures that would be required for the processing. A subsequent paper will report rheological properties of such plasticized sulfonated polysulfone materials.

2. Experimental

2.1. Materials

A disulfonated poly(arylene ether sulfone) random copolymer (BPS-XY) was used in this study (see Fig. 1) [3,5,7,8]; X indicates the molar percentage (mol%) of disulfonated monomer, and Y denotes the cation associated with the sulfonated groups and is either H (acid form) or K (potassium form). BPS-20K, having 20 mol% disulfonated monomer in the polymer backbone, was the focus of our studies. The BPS polymer was synthesized in the potassium form by Akron Polymer Systems (Akron, OH) following the synthetic procedure established by McGrath et al. [3,7,20,21] and was used as received. The acid or H form can be obtained by boiling BPS-K in sulfuric acid solution and then in de-ionized (DI water) [7]. Table 1 summarizes some characteristics of BPS-20K.

2.2. Plasticizer

Table 2 lists the physical properties of the PEG samples used in this study. These PEGs were purchased from Sigma Aldrich (PEG 200 Cat# P3015, PEG 300 Cat# 202371, PEG 400 Cat# 202398, PEG 600 Cat# 87333, St. Louis, MO) and were used as received.

2.3. Blend preparation

2.3.1. Solution casting method

For some of the studies reported here, solution casting was used as a convenient way to form films. A desired amount of BPS-20K/PEG was dissolved in N,N-dimethylacetamide (DMAc, Sigma Aldrich, Cat# 39940) to prepare a solution with 10 wt% solids. This solution was poured onto a glass plate and kept in an oven for 24 h at 60 °C and then in a vacuum oven for another 48 h to evaporate most of the DMAc [3,5,7]. Residual solvent was extracted by soaking this film in deionized (DI) water for 24 h and vacuum drying at 120 °C for 24 h [7]. Transparent films of uniform thickness (30–50 μm) were obtained and used for further characterization. To facilitate removal of the films from the glass plate, the glass plate was pretreated using a solution of chlorotrimethylsilane (Sigma Aldrich, Cat# 92361) and toluene (Sigma Aldrich, Cat# 650579) (70% by volume toluene) to render the surface of the glass hydrophobic.

2.3.2. DSM micro-compounding and compression pressing

Extruded samples of BPS-20K/PEG blends were prepared using a 5 ml twin screw micro-compounder (DSM Xplore, the Netherlands) and molded in a compression press (Wabash Metal Products Inc., Wabash, IN) to form films. The processing temperature was set to be at least 50–100 °C higher than the T_g of the blend and lower than the degradation temperature, T_d, and it was in the range of 170–210 °C. The desired quantities of BPS-20K and PEG were well mixed prior to feeding to the compounder and were extruded under an extra dry nitrogen atmosphere (99.9%, Matheson Tri-Gas, Austin, TX) to minimize degradation.

Table 1
Characteristics of BPS polymer.

Material	$\overline{M}_w$ [a] [g/mol]	IV[a] [ml/g]	T_g [b] [°C]	Water permeability[c] [L μm m^{-2} h^{-1} bar^{-1}]	NaCl rejection[c] [%]
BPS-20K	33,900	48.2	273	0.03	99.2

[a] Determined by SEC using NMP with 0.05 M LiBr at 50 °C.
[b] Measured by DSC, 20 °C/min.
[c] Table 1 from Ref. [3].

Table 2
Properties of PEG oligomers.

Material	Average M_n [g/mol]	Data obtained in this study		Literature data		
		T_g [a] [°C]	T_m [a] [°C]	T_g [b] [°C]	T_m [c] [°C]	Density[c] at 20 °C [g/cm^3]
PEG 200	200	−83	–	−86	−65	1.124
PEG 300	300	−76	−15	−78	−15 ~ −8	1.125
PEG 400	400	−72	2	−78	4–8	1.126
PEG 600	600	−69	17	−60	17–22	1.130

[a] Measured by DSC, 20 °C/min.
[b] PEG 200 from Ref. [14], PEG 300 from Ref. [22], PEG 400 from Refs. [15,16], PEG 600 from Ref. [23].
[c] Data reported in Sigma–Aldrich product documentation [24–27].

2.4. Thermal analysis

2.4.1. Differential scanning calorimetry (DSC)

DSC (Q100, TA Instruments, New Castle, DE) was used to measure the glass transition, T_g, and melting, T_m, temperatures of the various mixtures and components. For a typical experiment, a 5 mg sample of polymer was sealed in an aluminum pan, and a DSC thermogram was recorded under ultra high purity nitrogen (UHP 99.999%, Air Gas, Austin, TX) purge using a heating rate of 20 °C/min over the temperature range from −150 °C to 400 °C. The T_g was recorded as the midpoint of the heat capacity step change.

2.4.2. Dynamic mechanical analysis (DMA)

DMA (Q800, TA Instruments, New Castle, DE) was used to determine the T_g and the secondary transitions of the polymer systems. A film tension clamp was used with rectangular films of uniform thickness. The storage and loss moduli (G', G'') and damping factor (tan δ) were recorded over the temperature range from −150 °C to 400 °C at a heating rate of 2 °C/min and a frequency of 1 Hz under an ultra high purity nitrogen atmosphere.

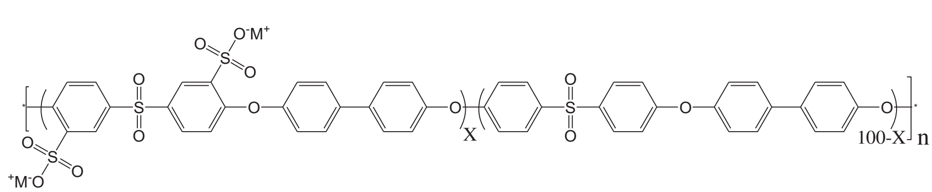

Fig. 1. Chemical structure of disulfonated poly(arylene ether sulfone) random copolymer: for BPS-XY series, X = mol% of disulfonated monomer ($0 < X < 100$), Y = H (acid form) or K (potassium salt form).

The T_g (°C) was determined as the temperature of the maximum loss tangent (tan δ_{max}).

2.4.3. Thermogravimetric analysis (TGA)

TGA (Q500, TA Instruments, New Castle, DE) was used to investigate sample weight changes as a function of time and temperature under an ultra high purity nitrogen atmosphere at a flow rate of 40 ml/min. A heating rate of 5 °C/min was used for the temperature ramp over the range from 25 °C to 600 °C. Isothermal scans were made by ramping the temperature to 230 °C at a heating rate of 20 °C/min and holding at this temperature for up to an hour.

2.5. Other characterization

2.5.1. Fourier transform infrared spectroscopy (FT-IR)

Attenuated Total Refection (ATR) FT-IR (Nicolet 6700 FT-IR Spectrometer, Thermo Scientific, Waltham, MA) was employed to probe for chemical structural changes after thermal treatment of PEG 200. For each measurement, 256 spectra were collected at a resolution of 4 cm^{-1}.

2.5.2. Proton nuclear magnetic resonance (^1H NMR)

^1H NMR spectra were recorded using a Varian DirectDrive spectrometer (Agilent Technologies, Santa Clara, CA) operating at 400 MHz to characterize chemical structure, number average molecular weights ($\overline{M}_n$) of the PEGs, degree of sulfonation of the BPS-20K, and concentration (wt%) of the PEGs in the BPS-20K/PEG blends. NMR samples were prepared by dissolving 20 mg of material in 2 cm^3 of $(CD_3)_2SO$, dimethyl sulfoxide-D6 (99.9%, Cat# DLM-10, Cambridge Isotope Laboratories, Andover, MA). ^1H NMR data were recorded under the following conditions: numbers of scans = 8, relaxation delay = 2 s, spin rate = 20 Hz.

2.5.3. Electrospray ionization (ESI)

ESI (Agilent 6530 Accurate-Mass QTOF LCMS, Agilent Technologies, Santa Clara, CA) in the positive mode was used to determine number ($\overline{M}_n$), and weight ($\overline{M}_w$) average molecular weight, as well as polydispersity (PDI) of the PEG materials. The carrier solvent was methanol, and the ion source temperature was 250 °C.

2.5.4. Sulfur elemental analysis

Sulfur elemental analysis was conducted at Galbraith Laboratories, Inc. (Knoxville, TN) to determine the polysulfone content in extruded blends with PEG. ASTM D4239-12 was used to measure the sulfur content in these samples.

3. Results and discussion

The melt processing temperature of a glassy polymer is typically at least 50–100 °C higher than its T_g and lower than temperatures that would result in significant polymer degradation during the time that the material was being processed. Based on this rule of thumb, since the T_gs of BPS polymers are in the range of 220–320 °C depending on the sulfonation level and ionic form [20], the minimum extrusion temperature range would be around 270–420 °C. However, because the sulfonated groups are susceptible to thermal degradation and the degradation temperature decreases with increasing sulfonation level [20], BPS polymers cannot be melt extruded. Therefore, extrusion of BPS requires a suitable plasticizer to lower the processing temperature range to well below the decomposition point.

Since PEG oligomers have been reported to be miscible with BPS [23], these materials are potentially attractive as plasticizers. Additionally, such oligomers are water soluble, which could permit water extraction of the PEG after melt extrusion [15,16]. The following results confirm the miscibility of PEG oligomers and BPS and explore a number of other questions (e.g., thermal stability, volatility of low molar mass PEG oligomers, etc.) related to extrusion of such blends.

3.1. Selection of BPS form

The potassium form of the sulfonated polysulfone, or BPS-K, was selected for use in this study. While the BPS-H form has a somewhat lower T_g than BPS-K [20], the acid form has a much lower degradation temperature than BPS-K. The better thermal stability of the K form in the potential melt processing temperature range (180–230 °C) is evident from the TGA scan presented in Fig. 2. Substantial weight loss in the BPS-H sample, presumably related to the onset of thermal degradation, begins at approximately 230 °C, which is much lower than the onset of significant weight loss in the BPS-K sample, which occurs above 400 °C.

BPS-20K (ion exchange capacity = IEC = 0.92 meq/g) was selected for this initial study since it has a good balance of thermal stability and membrane performance [3,5,8,20]; selected properties are listed in Table 1.

3.2. Thermal analysis of PEG

3.2.1. Plasticizer selection

PEGs are available with number average molecular weights spanning a very large range. However, low molecular weight PEGs, with $\overline{M}_n$ between 200 and 600 g/mol, are of particular interest for this study because they can depress the T_g of BPS-20K to the 100–150 °C range with relatively small amounts (<30 wt%) of plasticizer, and, being relatively small, they should be more rapidly removed, via leaching into water following melt processing, than higher molecular weight PEG materials. Furthermore, higher molecular weight PEGs are less effective for T_g depression, may be far more difficult to extract from the extruded blend with water owing to their large molecular size, and would contribute significantly to the blend viscosity.

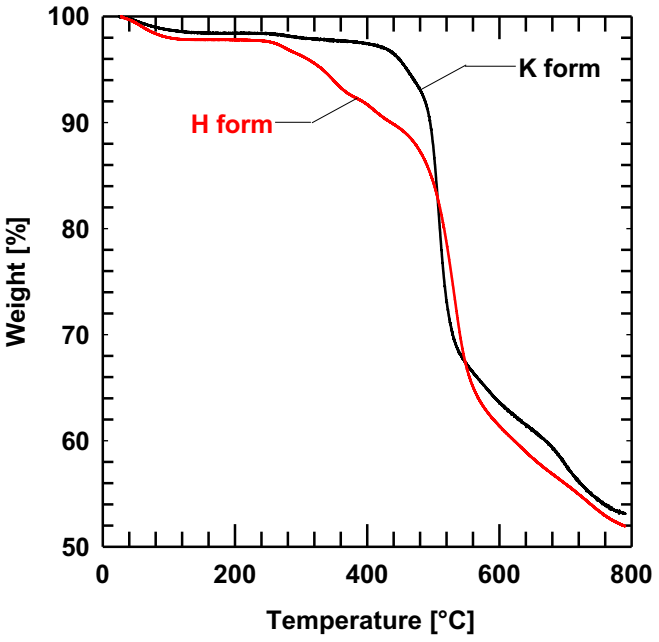

Fig. 2. Weight change of BPS-20K and BPS-20H as a function of temperature. The TGA scan was run in a nitrogen atmosphere with a ramp rate of 5 °C/min.

3.2.2. PEG Glass transition behavior

Estimation of the glass transitions of BPS/PEG blends requires accurate values of the T_g of each PEG considered. There is some literature on the T_g of PEG materials; however, the available data do not include all of the materials of interest to this study. Some papers report T_g values for PEG 200, 300 and 400 [14–16,22,28,29]. However, different methods to obtain T_g data were used in each report, so a consistent database cannot be assembled from the available literature sources for all of the materials considered in this study. Thus, we characterized the T_gs of the PEG 200–600 materials using DSC.

Fig. 3 presents first scan DSC thermograms of the PEG 200–600 materials. The sample preparation methods to obtain these data varied somewhat depending on the material. With no special sample preparation, PEG 200 and PEG 300 samples exhibit distinct glass transitions, and PEG 300 has a crystallization peak on heating above its T_g. However, with no special sample preparation, the PEG 400 and PEG 600 (or higher molecular weight PEG) samples do not show a distinct glass transition by DSC owing to their high level of crystallinity [28].

Therefore, the following procedure was used to obtain clear T_g values from DSC for the PEG 400 and 600 materials. Samples of PEG 400 and 600 were sealed in aluminum DSC pans at room temperature (i.e., above their melting points) and rapidly quenched in liquid nitrogen to prevent crystallization to the largest extent possible. Nevertheless, due to the extremely high crystallization rate of these materials, samples with some crystallinity were produced by this procedure; similar observations have been reported for torsion pendulum and NMR studies [28,30]. However, this technique does reduce the crystallinity enough to make a glass transition observable by DSC. After 1 h in liquid nitrogen, the samples were quickly moved to the DSC cell where the temperature had already been equilibrated at −150 °C, and a scan was run between −150 °C and 30–50 °C at a heating rate of 20 °C/min. The T_g was reported as the midpoint of the heat capacity step change during the first heat cycle. In the case of PEG 400 and 600 s and third cycles do not reveal any detectable glass transitions since all samples become highly crystalline after the first cycle; whereas, for PEG 200 and 300, the subsequent cycles overlap with the first cycle. Strong recrystallization exotherms are observed for PEG 400 and 600 in Fig. 3 at about −61 °C and −57 °C, respectively, and the beginning of a recrystallization exotherm is also observed in the PEG 300 sample.

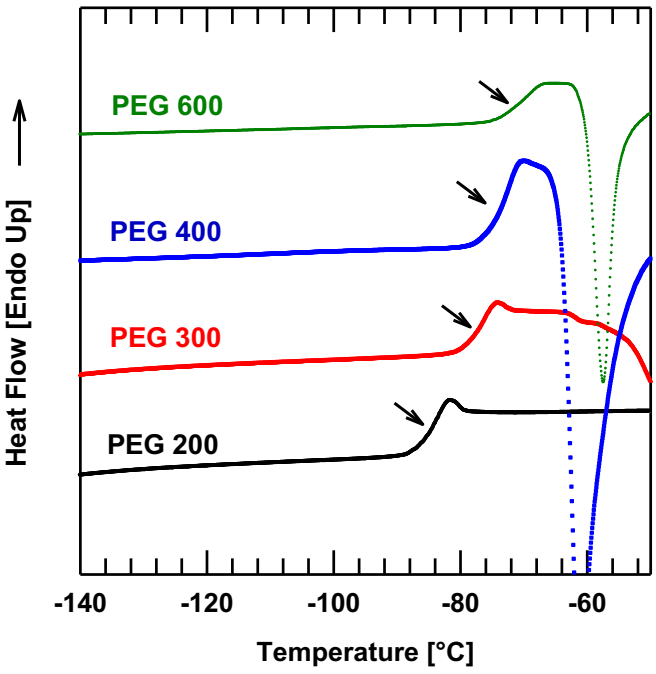

Fig. 3. First scan DSC thermograms of PEGs. The thermograms have been displaced vertically for clarity. The arrows denote the location of the glass transition temperatures.

The T_g and peak crystalline melting temperature, T_m, values from the first scan DSC thermograms are summarized in Table 2. The T_gs measured here are in a good agreement with the previous literature [14–16] and are used to predict the T_gs of BPS/PEG blends using the Fox equation [31]. After the glass transition (shown by the arrows in Fig. 3), crystallization occurred for PEG 300–600, followed by melting. The melting peaks are not shown in Fig. 3; however the T_m values detected here are similar to those given in the product literature, as shown in Table 2 [24–27].

In general, glassy polymers show a monotonic increase in T_g with increasing molecular weight up to a plateau value at high molecular weights [32,33]. As shown in Fig. 3, the PEG 200–600 samples exhibit this trend at least qualitatively. Faucher and others reported that higher molecular weight PEGs (greater than 4000 g/mol) do not follow this relation and have a maximum T_g at around 6000 g/mol [28,30]. This behavior is attributed to high crystallinity in these PEG materials, which restricts chain mobility in the amorphous phase, thereby influencing T_g. PEG crystallinity reaches a maximum in the range of 4000–30,000 g/mol [34], and above this range, the crystallinity drops significantly [28].

3.3. Glass transition of BPS-20K/PEG blends

The glass transition temperatures of BPS-20K/PEG blends were measured using both DSC and DMA. Before each DSC run, extruded BPS-20K/PEG blend samples were placed in aluminum DSC pans and kept under a nitrogen atmosphere at T_g + 10–20 °C for 10 min to remove any previous thermal history. Following this, the sample was cooled to −90 °C and scanned to 75–185 °C, depending on the blend composition, at a rate of 20 °C/min. This thermal cycle was repeated 3 times. The T_g (°C) was taken as the midpoint of the heat capacity step change during the third (and final) thermal cycle. In the case of DMA, the T_g (°C) was determined as the temperature of the maximum loss tangent (tan δ_{max}). DMA was used in addition to DSC because it is a sensitive method to verify T_g, as well as the secondary transitions of polymer segments, that might not be easily observable in DSC scans [30,35].

Thermograms of a mixture where one component is an amorphous polymer and the other is a semi-crystalline oligomer can reveal useful information about the physical state of the mixture such as the state of mixing in the amorphous phase and any crystallinity. Here the traditional criteria of a single T_g located between the T_gs of the individual components is adequate evidence for miscibility [36–38]. On the other hand, Lodge et al. claimed that some miscible blends such as PEO/PMMA containing low molecular weight PEG show two T_gs using DSC [22,29]. Other secondary transitions due to the water (−35 °C), etc. [30,39] can be seen as well and will be mentioned later.

Fig. 4 shows exemplary DMA and DSC scans for a series of BPS-20K/PEG 600 blends; similar data were observed for blends containing PEG samples with different molecular weights. The tan δ peak with the greatest intensity in the DMA scans, or the step change in heat capacity in the DSC scans, is associated with the T_g or α transition of the polymer mixtures. Both DSC and DMA scans exhibit a single composition-dependent T_g for the PEG concentrations considered (i.e., up to 40 wt%). The T_gs detected by DSC and DMA agree with each other within differences expected from these techniques and their characteristic time scales [35].

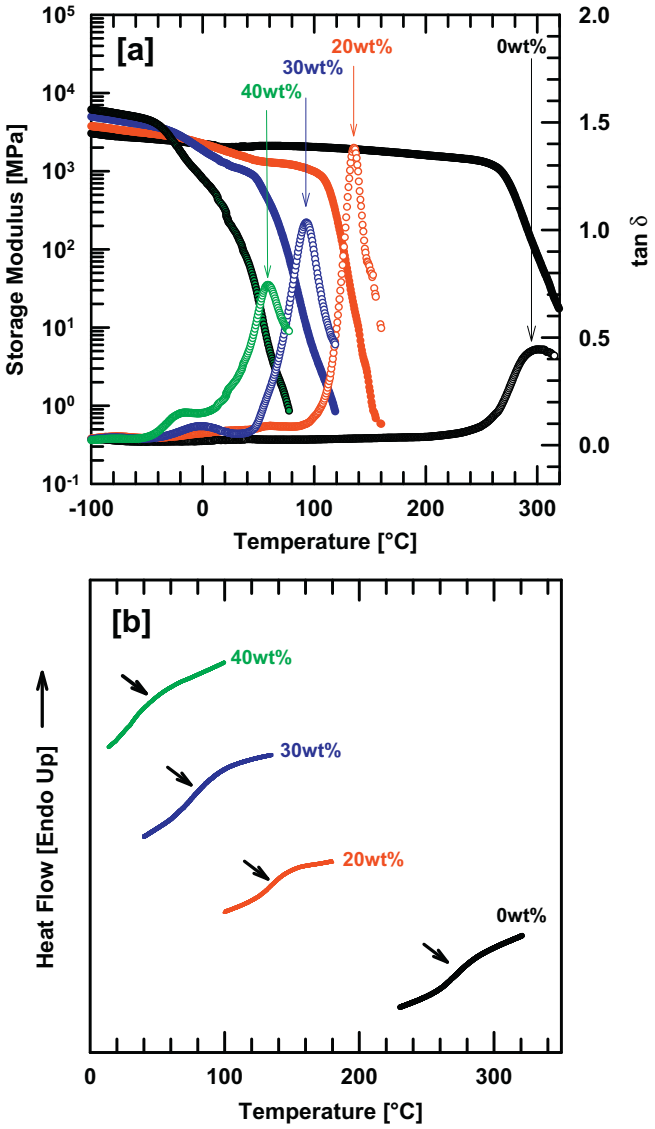

Fig. 4. [a] Dynamic mechanical analyses scans for BPS-20K/PEG 600 mixtures. (Frequency = 1 Hz, ramping rate = 2 °C/min) [b] Differential scanning calorimetric thermograms (final scan) of BPS-20K/PEG 600 blends. The DSC thermograms have been magnified vertically (magnification is different for each thermogram for easier viewing) and displaced along the vertical axis for clarity. The arrows identify the transitions selected as the glass–rubber transition in each blend.

The pure BPS-20K (i.e., BPS-20K/PEG 600 0 wt%) has a T_g of about 273 °C by DSC and 299 °C by DMA (see Table 3), and these values are somewhat higher than the previously reported values [20,23]. This difference can be explained by the different sample preparation procedures, and a similar observation has been reported by Xie et al. [7]. In our measurement, residual solvent was removed by soaking in DI water and vacuum drying; however, in the previously reported measurements, this solvent extraction process was not employed so some residual solvent may have remained in the sample, which would have lowered the T_g. Moreover, processing history (i.e., thermal treatment, filtering, etc.) as well as measurement method (i.e., ramp rate, sample size, etc.) can affect properties such as T_g [7,12,40].

Fig. 4a shows the storage moduli for all BPS-20K/PEG 600 0–40 wt% blends, with values in the range of 3000–5000 MPa at low temperatures, followed by a sharp decrease, characteristic of a glass-to-rubber transition, while a corresponding maximum in tan δ occurs in the same range. As the PEG concentration (wt%) increases, the characteristic decrease in storage modulus and the peak in tan δ progressively shift to lower temperature, indicating T_g depression as expected for a plasticizer [23,41–43].

Table 3
The onset, mid- and end- temperatures of heat capacity step change (DSC) and the temperatures where loss modulus (G'') and tan δ reach their maximum (DMA) at the glass transition of BPS-20K/PEG 600 blends. The mid temperature is used to report the T_gs of the blends for DSC. In the case of DMA, the T_g was determined as the temperature of the maximum loss tangent (tan δ_{max}).

PEG 600 [wt%]	DSC				DMA	
	Onset temp [°C]	Mid temp [°C]	End Temp [°C]	ΔT_g[a] [°C]	Temp at G''_{max} [°C]	Temp at tan δ_{max} [°C]
0	256	273	288	32	273	299
20	122	132	147	25	112	131
30	64	75	94	30	58	93
40	38	43	54	16	–[b]	58

[a] ΔT_g [°C] = $T_{end\ temp} - T_{onset\ temp}$.
[b] Not distinguishable.

Interestingly, the tan δ peak for the mixture containing 20 wt% PEG 600 is quite sharp. However, as more PEG is added to the blend, the peak decreases in height and becomes broader in width. This flattening and broadening effect has been reported for a number of polymer blends and plasticized polymers including poly(vinyl chloride) (PVC) and polystyrene (PS), etc. [36,44,45]. This broadening has been attributed to local concentration fluctuations [36,37,41,44–49]. Since the time scale of these fluctuations is longer than the time needed for chain segmental motion, the relaxing segments are likely to encounter varying local environments and, thus, relax at different rates. As a result, the DMA profile reflects a broad range of local relaxation processes [36,37].

Some secondary or sub-T_g relaxation processes are evident in the range between −50 °C and −25 °C. This transition is not seen in pure BPS-20K but appears in all mixtures with PEG 600. At 20 wt% PEG, this relaxation is very small. However, as more PEG is added to the blend, the intensity of this tan δ peak increases and seems to shift to the lower temperatures. This peak may be related to moisture absorbed by the hygroscopic PEG and/or to some relaxation associated with PEG [30,39,49–53].

Table 3 presents the onset, mid- and end- temperatures of the heat capacity step change (DSC) and the temperatures where the tan δ reaches its maximum (DMA) at the glass transition of BPS-20K/PEG 600 blends as described in Fig. 4.

Fig. 5 summarizes the effect of PEG concentration and molecular weight on the T_gs of BPS-20K/PEG blends. The T_gs determined by DSC were used for this analysis since the PEG T_gs were detected with DSC because of difficulties when measuring liquid samples using DMA [30], so it was consistent to employ DSC T_gs for further analysis. As the PEG concentration increases, the blend T_g is depressed (see Fig. 5a). Two potential reasons for this decrease are: (1) the PEG adds more free volume to the polymer matrix, which would reduce interchain restrictions on polymer segmental mobility, and (2) PEG interactions with the ionic groups in BPS could reduce ionic interactions of the sulfonated groups in BPS-20K [23,41,43]. The dashed lines, shown in Fig. 5a, represent the prediction of the Fox equation [36]:

$$\frac{1}{T_g} = \frac{w_1}{T_{g1}} + \frac{w_2}{T_{g2}} \quad (1)$$

where w_1, T_{g1}, w_2 and T_{g2} are the weight fractions and glass transition temperatures of BPS-20K and PEG, respectively [31]. As shown in Fig. 5b, at a fixed PEG concentration, the blend T_g is slightly lower at lower PEG molecular weight. This result is

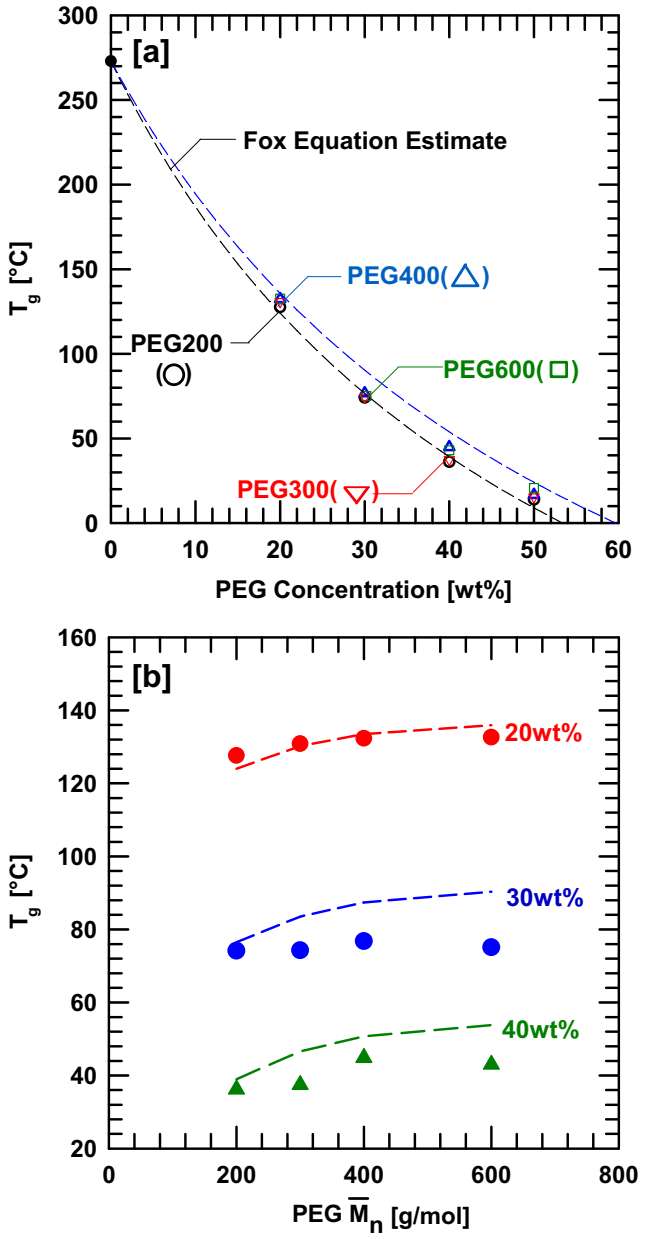

Fig. 5. Effect of PEG $\overline{M}_n$ and concentration on T_g of BPS-20K/PEG blends. T_gs were measured using DSC: [a] effect of PEG concentration (wt%) and [b] effect of the PEG $\overline{M}_n$ (g/mol) on T_g of BPS-20K/PEG blends. Dashed lines are the Fox equation estimates. In [a], dashed lined are the Fox equation estimates of BPS-20K/PEG 200 (lower) and BPS-20K/PEG 600 (upper). The Fox equation estimates for PEG 300 and PEG 400 lie between those of PEG 200 and PEG 600 and are not shown for easier viewing.

reasonable given the influence of PEG molecular weight on the T_g of PEG (see Table 2) [48]. The dashed lines in Fig. 5b are also predictions of the Fox equation, calculated using the known T_g values of the BPS-20K and PEG as well as their concentrations in the blend.

3.4. Thermal stability of BPS-20K during extrusion conditions

Based on the T_g values obtained in the blends and the rule of thumb that melt processing is performed 50–100 °C above the T_g, the highest melt processing temperature needed would be in the range of 230 °C, based upon the T_g of BPS-20K plasticized with 20 wt% of PEG 600 (see Fig. 5b). Of course, the melt processing temperature could be lower, if more plasticizer or lower molecular weight plasticizer was used. Consequently, it was of interest to explore the thermal stability of these BPS-20K/PEG blends.

BPS-20K exhibits good thermal stability at the temperature of interest. For example, Fig. 6 presents the mass loss of a sample of BPS-20K as a function of time in a TGA experiment. In this particular experiment, the temperature of the sample was increased at 20 °C/min to 230 °C and then held at 230 °C for 60 min under nitrogen atmosphere. There is a slight mass loss initially, which may well be due to traces of water remaining in this hydrophilic material. However, the mass is very nearly constant during the isothermal hold at 230 °C.

3.5. Thermal stability of PEGs: TGA

There is a significant literature on the thermal and chemical stability of PEGs for applications in various fields, including energy storage materials, biomedical engineering, and archeology [54–57]. The time scale of thermal stability in these applications is much longer (a week to several years) relative to extrusion, which takes only a few minutes. Thus, the temperature range, PEG molecular weight, and environmental conditions considered in previous studies of thermal and chemical stability were quite different from the relevant conditions in this study [57–63]. Therefore, the thermal stability of low molecular weight PEGs of interest for this study was investigated.

At high temperatures in air, the hydroxyl groups in PEG are readily attacked by oxygen to form hydroperoxide radicals. Random chain scission then proceeds, producing many oxygenated products [54,55,58,59,61,62]. For this reason, lower molecular weight PEG materials degrade faster since more hydroxyl groups exist per unit mass, and, thus, peroxides are formed faster. For the non-oxidative thermal degradation, depolymerization or decomposition takes place when the main chain backbone is broken by ether cleavage, leading to radical or non-radical scission [57]. In either case, the hydroxyl groups are susceptible to degradation.

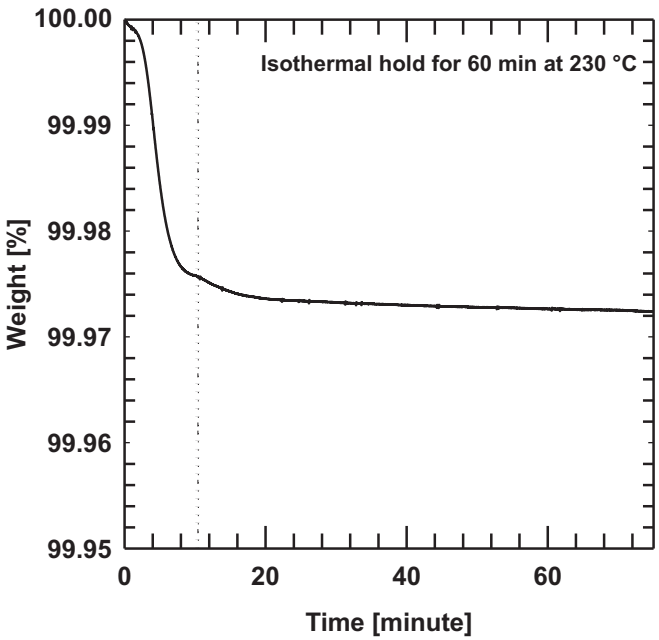

Fig. 6. Weight change of BPS-20K as a function of time under nitrogen atmosphere. The sample was heated from ambient to 230 °C at a heating rate of 20 °C/min and was then held isothermally at 230 °C for 60 min. The dashed line represents the time with the temperature reached 230 °C.

One way to probe the thermal stability at elevated temperatures is via TGA experiments. The weight change of PEG materials as a function of temperature is shown in Fig. 7a. As molecular weight increases, the temperature where the mass loss becomes significant increases. However, this mass loss could result from either degradation or evaporation. Similar observations apply when the PEG materials are held isothermally at 230 °C for 30 min in the TGA, as shown in Fig. 7b. PEG 200 mass decreases to 50% of the initial value during the temperature ramp to reach 230 °C mainly because of evaporation, as will be discussed further below. Consequently, it is difficult to determine the mass loss due to degradation during the hold at 230 °C. As a result, methods other than TGA are needed to assess the thermal stability of PEGs at various temperatures and times.

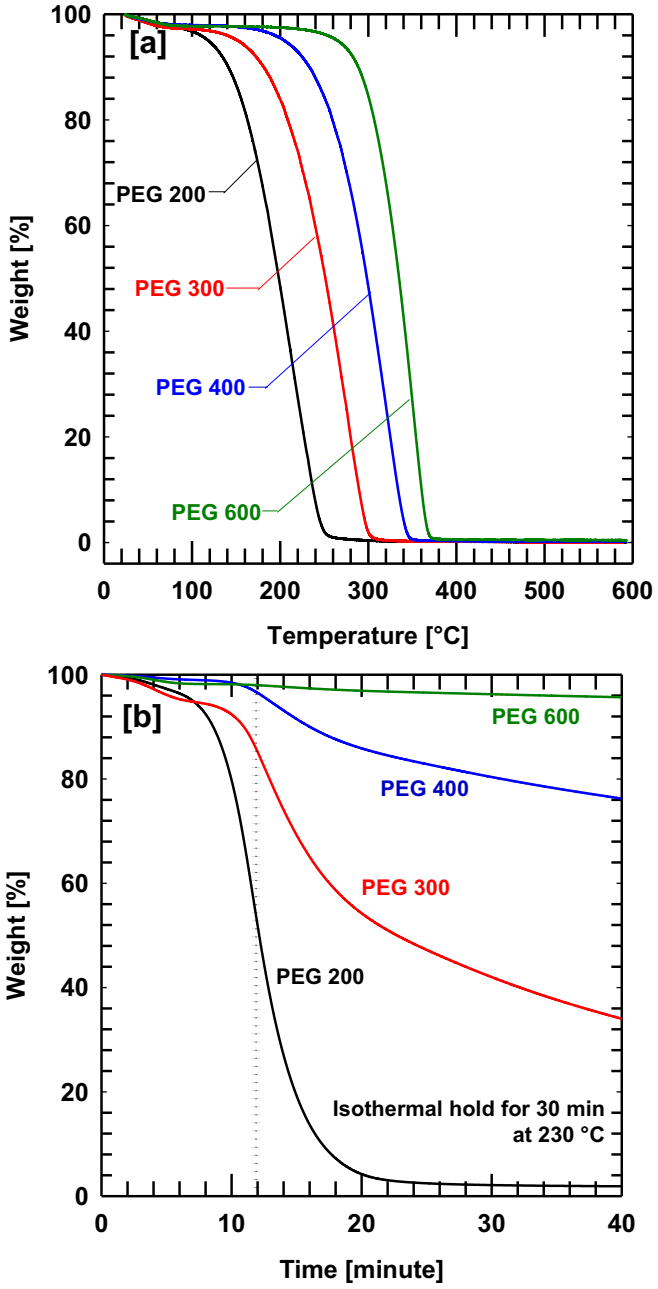

Fig. 7. Mass loss of PEGs of various molecular weights in a nitrogen atmosphere. [a] The weight change as a function of temperature at a ramp rate of 5 °C/min. [b] The weight change as a function of time. The temperature was ramped from ambient to 230 °C at 20 °C/min and then held at 230 °C. The vertical dashed lines shows the time when the temperature first reached 230 °C.

3.6. Thermal stability of PEG 200

PEG degradation, with or without oxygen, may cause random chain scission and result in low molecular weight products. As a result, the chemical structure is changed, the molecular weight is decreased, polydispersity (PDI) is increased, and the T_g, T_m and heat of fusion are reduced [30,54,55,57,58]. A major difference between oxidative and non-oxidative degradation of PEG lies in the products formed [30,57,58]. These aspects were tested by different characterization techniques to understand the thermal stability of PEG 200 at extrusion conditions.

PEG samples were held at high temperatures, in the range of 170–250 °C, for times ranging from 10 to 30 min, in a rheometer (AR2000EX from TA Instruments, 25 mm EHP parallel plate, gap distance of 1 mm) in both nitrogen and air atmospheres. A rheometer was used since it offered accurate control of isothermal hold and environmental conditions. A minimum time of 10 min was chosen since the approximate sample residence time at high temperature in the compounder and compression press used to prepare the blend samples was less than 10 min. PEG 200 is the least stable of the PEGs of interest, so it was selected for study. If PEG 200 is stable under the most aggressive thermal conditions of interest for this study, other higher molecular weight PEG materials should be stable as well. Characteristics such as number average molecular weight ($\overline{M}_n$), molecular structure, polydispersity (PDI), etc. after the isothermal hold were investigated to ascertain thermal stability.

3.6.1. Thermal stability under nitrogen

3.6.1.1. FT-IR: chemical structure. FT-IR was used to detect chemical structural changes by tracking characteristic absorption bands. Fig. 8 shows the FT-IR spectra (4000–500 cm^{-1}) of PEG 200 after holding isothermally for 10–30 min at temperatures ranging from 220 to 250 °C under nitrogen.

No significant changes were observed in the PEG 200 spectra after holding at 230 °C for 30 min or at 250 °C for 10 min. However, after holding for 30 min at 250 °C, a stretching vibration for carbonyl groups at 1710–1750 cm^{-1} appears (shown by the arrows in Fig. 8), which is likely due to aldehyde formation. Similar

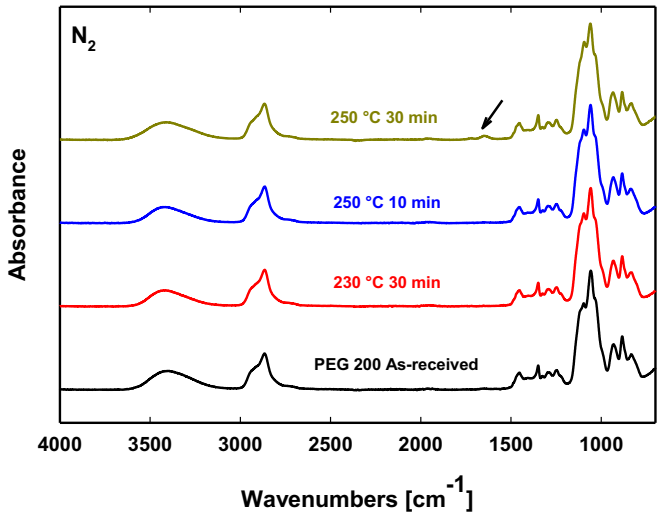

Fig. 8. FT-IR (ATR mode) spectra of PEG 200 exposed to various temperatures and times under nitrogen. FT-IR spectra were placed vertically for easier viewing. The arrows denote a stretching vibration for carbonyl groups at 1710–1750 cm^{-1}.

observations were reported by Pielichowski et al. using TG/FT-IR and TG/MS; in the early stages of non-oxidative thermal degradation (350–410 °C), the main absorption bands are from C=O stretching (from aldehyde, 1750 cm^{-1}) along with other volatile products such as C=O (from CO_2, 2320 cm^{-1}), C=C (from alkenes, 1600 cm^{-1}), and OH groups (from alcohols and ethers, 1140 cm^{-1}) [57]. However, here the absorbance associated with the carbonyl stretching is small, so no characteristic band other than this stretching was seen. This result is reasonable because the isothermal hold temperature was only 250 °C, which is 100–150 °C lower than the degradation temperature mentioned in the literature. In subsequent ^{1}H NMR studies, this sample does not exhibit any characteristic peaks from aldehydes, and the molecular weight is in a similar range to that of as-received PEG 200. (Details will be explained in the subsequent section.)

Based on the FT-IR analysis, PEG 200 seems stable up to 230 °C for 30 min or 250 °C for 10 min in a nitrogen atmosphere.

3.6.1.2. ^{1}H NMR: molecular structure and $\overline{M}_n$. ^{1}H NMR was employed to verify the molecular structure of PEG 200 and to calculate the $\overline{M}_n$ before and after holding isothermally at various temperatures for various times. The peak assignments of PEGs in $(CD_3)_2SO$ are presented in Fig. 9 and numbers next to each peak are the integrated ratios of the proton peaks. For PEG 200, the $\overline{M}_n$ was determined by the ratios of proton peaks at: (a) $\delta = 4.56$ ppm (2H, –OH groups), (b) $\delta = 3.39$ ppm and (c) $\delta = 3.46$ ppm (4H, external CH_2–CH_2–O), (d) $\delta = 3.49$ ppm ($4(n-2)$H, internal $-(CH_2-CH_2-O)_{n-2}-$). Therefore, the integral H_b ($\delta = 3.39$ ppm) should be identical to the integral H_c ($\delta = 3.46$ ppm), and it should be twice the integral H_a ($\delta = 4.56$ ppm). Based on this relationship, the number of repeat units, n, in the polymer chain was calculated as follows:

$$n = \left\{ \frac{\left(\int H_d + \int H_c \right) - \int H_b}{4} \right\} + 2 \quad (2)$$

$\overline{M}_n$ was calculated as follows:

$$\overline{M}_n = (n \times 44) + 18[\text{g/mol}] \quad (3)$$

Based on this analysis, as-received PEG 200 has a $\overline{M}_n$ value of 210 g/mol.

Table 4 presents the $\overline{M}_n$s determined by ^{1}H NMR for an as-received PEG 200 sample and for samples exposed, under nitrogen, for two times (i.e., 10 and 30 min) at two different temperatures, 230 °C and 250 °C. After holding under nitrogen, the $\overline{M}_n$ is slightly increased with longer time and higher temperature exposure. This change is likely due to the selective evaporation of small molecular weight components and details will be explained with ESI and DSC results in the following section. The ^{1}H NMR spectra of these samples, which are not shown for the sake of brevity, were quite similar to that of the as-received sample.

After holding PEG 200 at 250 °C for 30 min under nitrogen, a stretching vibration for carbonyl groups is observed in FTIR at 1710–1750 cm^{-1} (see Fig. 8). However, there is no evidence of aldehyde or other oxygenated products by ^{1}H NMR. The amount of by-product may be very small so it could not be detected by ^{1}H NMR, considering the sensitivity of two different techniques [64]. Even though the amount of by-product is very small, extrusion conditions involving holding a sample at 250 °C for 30 min will not be included in future studies to prevent any possible degradation.

3.6.1.3. ESI and DSC: $\overline{M}_n$, PDI and T_g. When PEG degrades, random chain scission reduces the polymer chain length and produces low molecular weight products. Therefore, $\overline{M}_n$ is decreased, and the polydispersity (PDI) is broadened. The low molecular weight products also lower T_m and the heat of fusion, as much as 13 °C and 32 J/g, respectively [54,57]. The T_g is also reduced by thermal degradation since the polymer chain length is shortened, and low molecular weight products act as plasticizers. For example, in HDPE, after 3 days of aging at 120 °C in air, the T_g is depressed from −106 °C to −116 °C [30].

However, Bigger et al. reported that by DMA, PEG ($\overline{M}_n = 100{,}000$ g/mol) exhibits little change in T_g after holding in air for 26 h at 120 °C. A noticeable increase in the area under the tan δ curve appears as oxidization proceeds because this area indicates the amorphous portion of the polymer, but T_g was only slightly changed. They explained these observations in terms of the competing effects of chain scission and crosslinking, which shift the

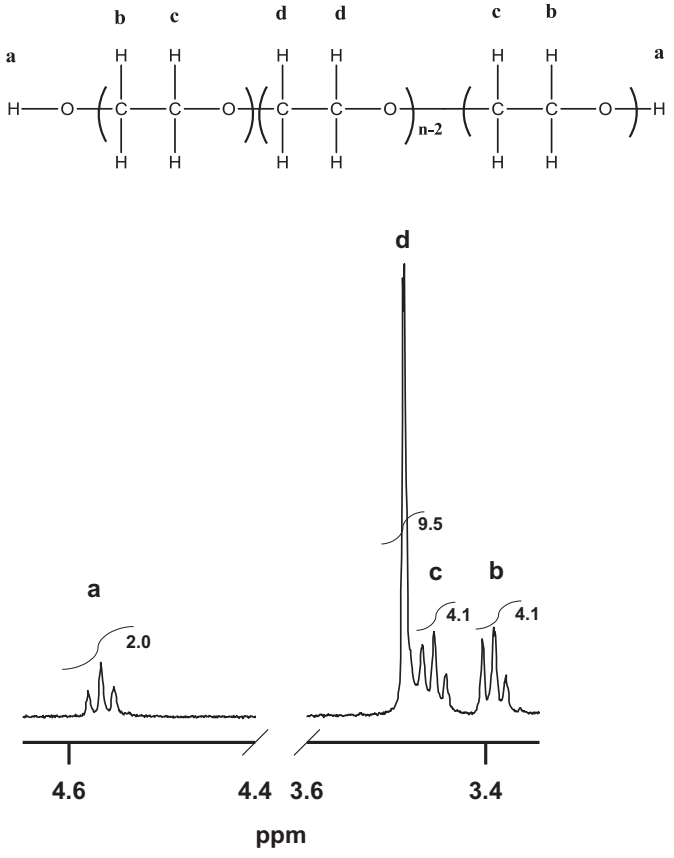

Fig. 9. ^{1}H NMR spectra of as-received PEG 200. The numbers next to each peak are the integrated ratios of proton peaks.

Table 4
$\overline{M}_n$, PDI and T_g of as-received PEG 200 and PEG 200 following isothermal holds at various temperatures and times in a nitrogen atmosphere.

PEG 200	$\overline{M}_n$[a] [g/mol]	Highest intensity M_n[b] [g/mol]	$\overline{M}_n$[b] [g/mol]	PDI[b]	T_g[c] [°C]
As-received	210	190	230	1.04	−83
230 °C, 10 min, N_2	210	240	260	1.04	−81
230 °C, 30 min, N_2	230	240	260	1.04	−80
250 °C, 10 min, N_2	230	240	250	1.04	−79
250 °C, 30 min, N_2	260	280	270	1.03	−79

[a] Determined by ^{1}H NMR.
[b] Determined by ESI.
[c] Determined by DSC, 20 °C/min.

T_g in opposite directions. Still large scale crosslinking, i.e., forming a microgel, was not observed, so they suspected a loose crosslinked network might form due to oxidation [30]. In contrast, PEG aged at 60 °C (below its T_m) changes from a free-flowing powder to a waxy solid, suggesting a decrease in T_g owing to random chain scission [30,65]. Although many previous studies agree that thermal degradation leads to chain scission and produces low molecular weight products, it is also important to confirm whether crosslinking occurs under the extrusion conditions of interest for this study.

Since PEG 200 does not exhibit a T_m, its glass transition after thermal exposure was measured using DSC, and $\overline{M}_n$ was calculated from ^{1}H NMR and ESI data. The $\overline{M}_n$ s measured using both approaches are usually in good agreement. Since ESI also gives the relative intensities of different molecular weight species in a sample, the PDI can be estimated. If crosslinking occurs during thermal treatment, high molecular weight products should be observed, so ESI analysis provides a tool for assessing crosslinking.

Fig. 10 shows the ESI spectrum of as-received PEG 200. A standard ESI result provides the relative intensity (area) versus mass-to-charge (m/z) as shown in Fig. 10. From this data, $\overline{M}_n$, $\overline{M}_w$ and PDI are calculated as follows:

$$\overline{M}_n = \frac{\sum M_i \cdot N_i}{\sum N_i} \tag{4}$$

$$\overline{M}_w = \frac{\sum M_i^2 \cdot N_i}{\sum M_i \cdot N_i} \tag{5}$$

$$\mathrm{PDI} = \frac{\overline{M}_w}{\overline{M}_n} \tag{6}$$

where M_i is calculated as $m/z - 23$, since z is usually 1 and the mass of Na^+, an adduct ion, should be subtracted, and N_i corresponds to the relative intensity. From this equation, $\overline{M}_n$ and $\overline{M}_w$ were determined to be 230 g/mol and 240 g/mol, respectively, so the PDI is 1.04.

PEG 200 has a nominal molecular weight of 200 (the average number of repeating unit is 4–5; if $n = 4$, $\overline{M}_n = 194$ g/mol, if $n = 5$, $\overline{M}_n = 238$ g/mol) based on the manufacturer's specification. The $\overline{M}_n$ values determined by ^{1}H NMR (210 g/mol) and ESI (230 g/mol) are consistent with this specification within the uncertainty of the measurements. The PDI is around 1.04, meaning a narrow molecular weight distribution typical of a living polymerization method [66].

Fig. 11 presents DSC thermograms of PEG 200 after isothermal holds in nitrogen, and Table 4 summarizes M_n, PDI and T_g, measured by ^{1}H NMR, ESI and DSC, respectively. After isothermal holds, the $\overline{M}_n$ and T_g are observed to increase slightly with longer time or higher temperature exposure, while the PDI remains low (1.03–1.04). This is due to the evaporation of low molar mass constituents and is confirmed by comparing ESI spectra after isothermal holds.

Fig. 12 shows ESI spectra for PEG 200 after isothermal holds under a nitrogen atmosphere. The intensities of different molecular weights are normalized by the highest molecular weight (238 g/mol) to compare the relative ratio of each molecular weight constituent between samples. As shown in Fig. 12a, when PEG 200 was held at 230 °C, the molecular weight distribution shifts somewhat to higher molecular weights, most likely because the low molecular weight oligomers evaporate during the isothermal hold. Fig. 12b shows an enlargement of the molecular weight range between 100 and 200 g/mol. The amount of low molecular weight materials is sharply reduced after the isothermal holds compared to that of as-received PEG 200.

The results are consistent with selective evaporation of low molar mass constituents. NMR and FT-IR do not show any strong changes in chemical structure upon exposure to these temperature/time combinations under nitrogen. $\overline{M}_n$ increases somewhat with longer time or higher temperature exposure, which is consistent with the loss of low molecular weight species during the

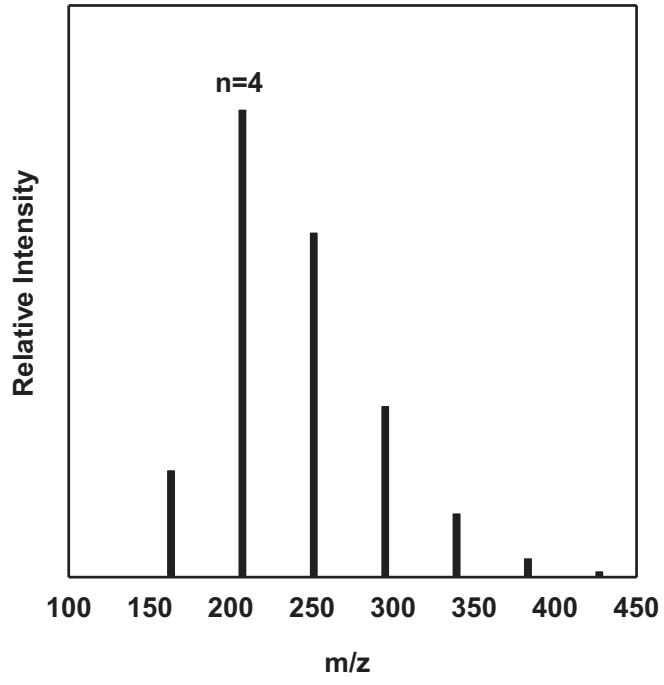

Fig. 10. Electrospray ionization (ESI) spectrum of as-received PEG 200. The peak at $m/z = 217$ corresponds to 4 repeat units, (i.e., $n = 4$), which corresponds to a molecular weight of 194 g/mol. For clarity, signals from noise were not included in this plot.

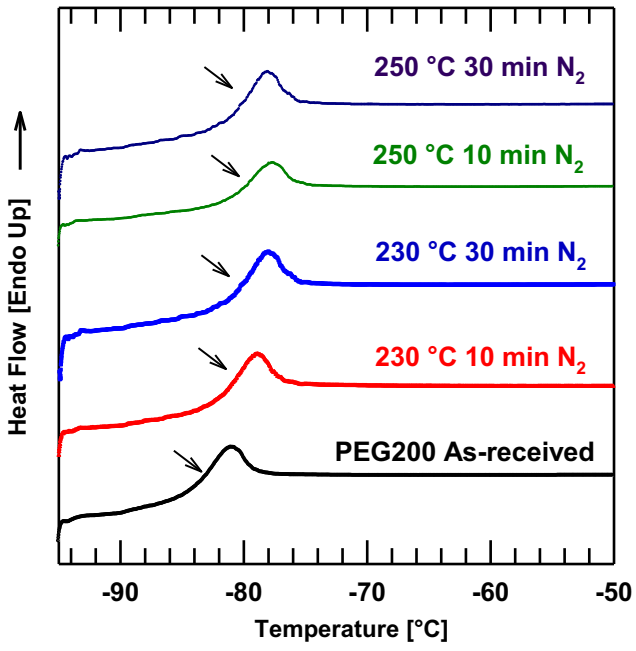

Fig. 11. DSC thermograms of PEG 200 after the isothermal holds at various temperatures and times in a nitrogen atmosphere. The thermograms have been displaced vertically for clarity. The arrows denote the location of the glass transition temperatures.

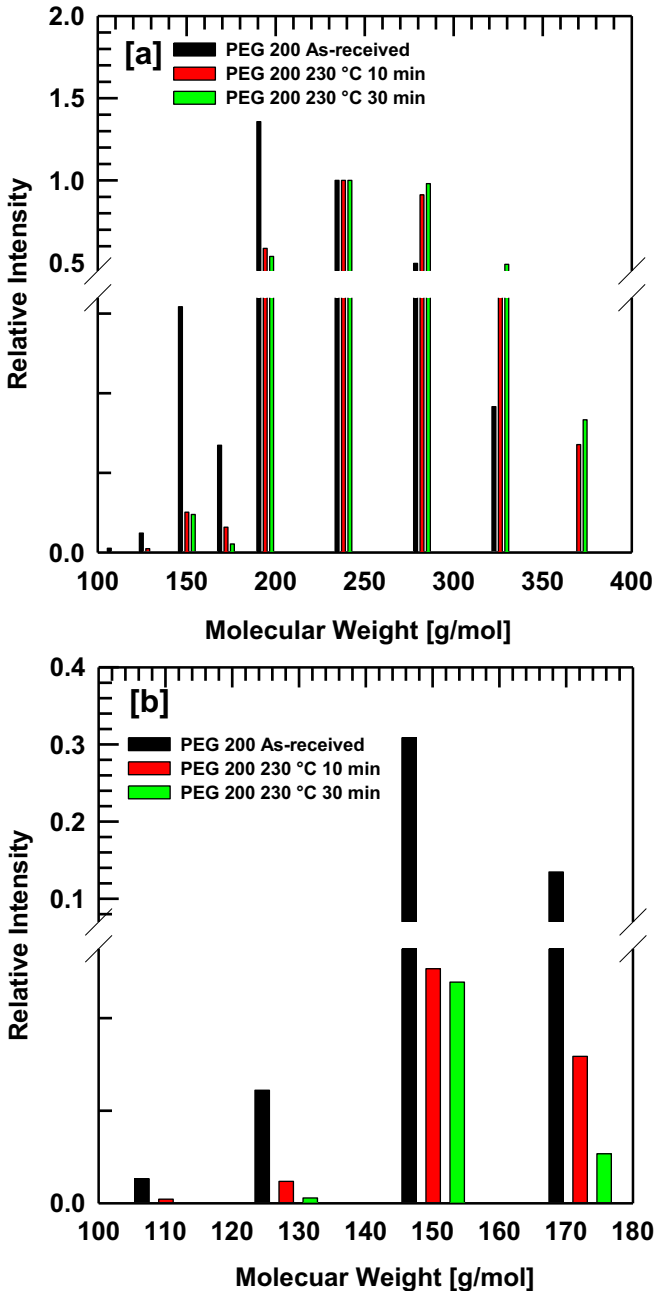

Fig. 12. ESI spectra of PEG 200 after isothermal holds at various temperatures and times under nitrogen. [a] The molecular weight range between 100 and 400 g/mol and [b] between 100 and 200 g/mol.

isothermal hold. The T_g increases slightly, which would also be consistent with loss of low molecular weight molecules via evaporation. The PDIs remain similar (1.03–1.04) or perhaps become slightly smaller at the highest temperature and longest exposure time, which would also be consistent with the selective evaporation of low molecular weight species. While some longer chain species may also evaporate, it is presumed that the smaller species would evaporate more rapidly, and the results are consistent with this hypothesis.

Therefore, chain scission is not significant for PEG 200 during isothermal holds in a nitrogen atmosphere. Also crosslinking is not likely to occur since no higher molecular weight species were found in the ESI spectra, PDI values were changed little, and the $\overline{M}_n$ was in a similar range of 230–270 g/mol (although there was a slight increase due to selective evaporation as mentioned earlier). All of these results suggest little, if any, degradation for the PEG 200 at these conditions. (Still, the extrusion condition of 250 °C for 30 min will not be included for future studies due to the FT-IR results.)

3.6.2. Thermal stability in air

3.6.2.1. FT-IR: chemical structure. Following thermal exposure in air, shown in Fig. 13, the change in the spectrum is more obvious because of oxidation. Because PEG 200 was held at higher temperatures and for longer times, the intensity of the C=O stretching peak (1710–1750 cm^{-1}) becomes greater, which may originate from degradation-induced formation of aldehyde or other oxygenated products containing ketone [54,57,58]. Based on the FT-IR analysis, PEG 200 seems stable up to 220 °C for 10 min in air.

3.6.2.2. ^1H NMR: molecular structure and $\overline{M}_n$. The ^1H NMR spectrum after holding a sample in air at 220 °C for 10 min is also identical to the spectrum of as-received PEG 200 (see Fig. 9). However, as shown in Fig. 14, after holding at 250 °C for 30 min in air, many additional peaks can be seen in the spectrum. In the FT-IR of the sample held at these conditions, a distinct C=O stretching peak appeared. The chemical structure was no longer identical to that of as-received PEG 200 and, thus, $\overline{M}_n$ cannot be calculated from the NMR results. Oxygenated by-products may have been generated [30,57,58]; further investigation would be required to identify these by-products and this is not an objective of this study.

3.6.2.3. ESI and DSC: $\overline{M}_n$, PDI, and T_g. Fig. 15 presents DSC thermograms of PEG 200 after isothermal holds in air and in nitrogen, and Table 5 summarizes $\overline{M}_n$, PDI and T_g, measured by ^1H NMR, ESI and DSC, respectively. Similar to the results under nitrogen, the $\overline{M}_n$ and T_g values increase slightly while PDI exhibited little change, indicating the selective evaporation of low molar mass constituents.

For the temperature range of 220–230 °C, there is no difference in terms of the molecular structure, $\overline{M}_n$, T_g and PDI between PEG 200 that was isothermally held for 10 min in air and in nitrogen. This implies good potential thermal stability during melt processing of PEG 200 at temperatures up to 220 °C for at least 10 min without a nitrogen blanket.

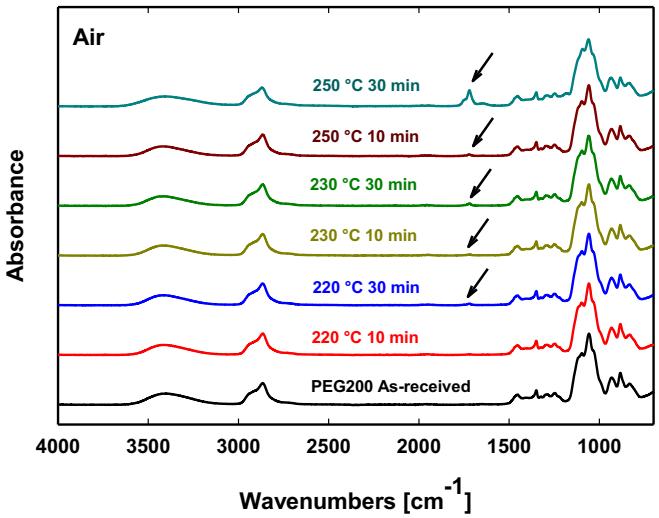

Fig. 13. FT-IR (ATR mode) spectra of PEG 200 exposed to various temperatures and times in air. FT-IR spectra were placed vertically for easier viewing. The arrows denote a stretching vibration for carbonyl groups at 1710–1750 cm^{-1}.

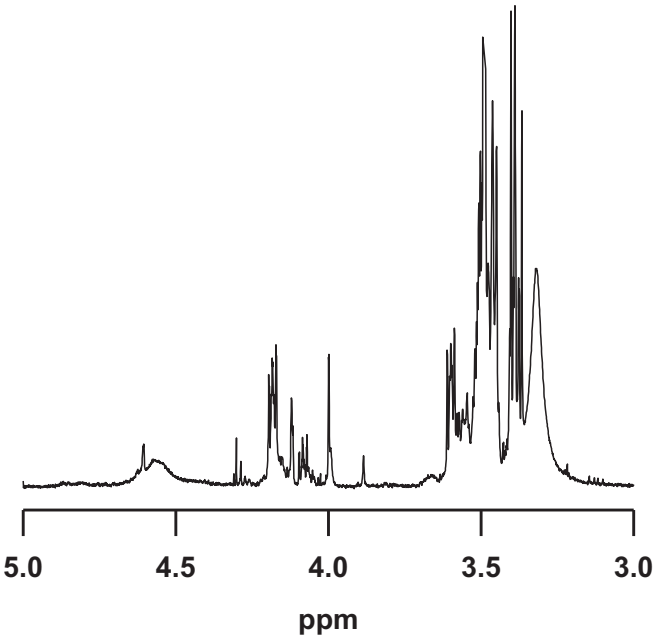

Fig. 14. ^{1}H NMR spectra of PEG 200 after isothermal holding at 250 °C for 30 min in air.

Based on results from these studies, PEG 200 is stable up to 250 °C for 10 min or 230 °C for 30 min under a nitrogen atmosphere and up to 220 °C for 10 min in air. Accordingly, higher molecular weight PEGs, such as PEG 300–600, should be stable within this temperature/time ranges as well.

3.7. Thermal stability of PEG 200 following compounding and film pressing

BPS-20K/PEG 200 blends were prepared using a DSM micro-compounder and a compression press using the processing

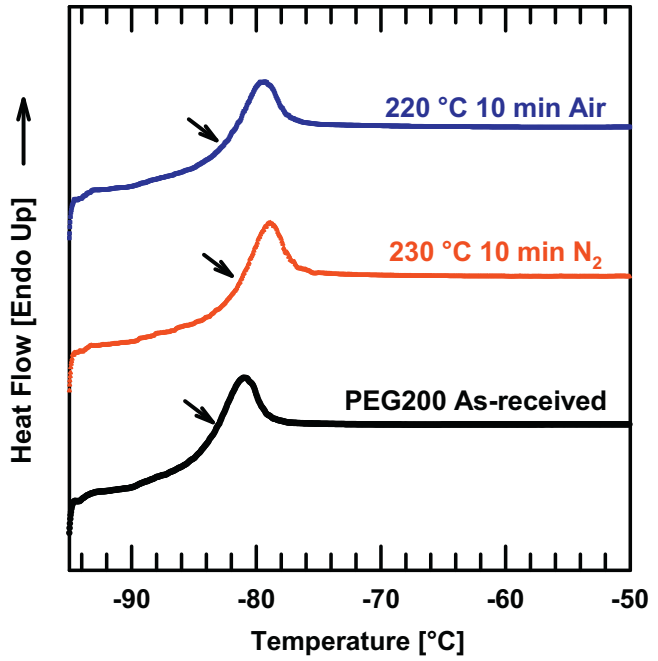

Fig. 15. DSC thermograms of PEG 200 after isothermal holds at various temperatures and times under nitrogen atmosphere and in air. The thermograms have been displaced vertically for clarity. The arrows denote the location of the glass transition temperatures.

Table 5
$\overline{M}_n$, PDI and T_g of PEG 200 after isothermal holds at various temperatures and times under nitrogen atmosphere and in air.

PEG 200	$\overline{M}_n$[a] [g/mol]	Highest intensity M_n[b] [g/mol]	$\overline{M}_n$[b] [g/mol]	PDI[b]	T_g[c] [°C]
As-received	210	190	230	1.04	−83
230 °C, 10 min, N_2	210	240	260	1.04	−81
220 °C, 10 min, Air	210	240	260	1.03	−81

[a] Determined by ^{1}H NMR.
[b] Determined by ESI.
[c] Determined by DSC, 20 °C/min.

temperature range identified. To confirm whether blending or melt processing induced any thermal degradation, the molecular structure, the PEG $\overline{M}_n$, and the PEG content of the extruded samples were analyzed using ^{1}H NMR and sulfur elemental analysis.

^{1}H NMR was used to determine the molecular structure of PEG and BPS-20K (especially the degree of sulfonation), the PEG $\overline{M}_n$ and the PEG concentration (wt%) in the extruded samples. All extruded samples were analyzed by ^{1}H NMR. However, in Fig. S1 (see Supplemental Material), only the BPS-20K/PEG 200 60 wt% sample is shown since the sample containing 60 wt% PEG is expected to be the least stable among the extruded samples in terms of the evaporation and thermal degradation during melt processing.

The molecular structure of PEG 200 is not changed, as shown in Fig. S1-a, and no peaks for oxygenated products are observed. The PEG $\overline{M}_n$ was determined using the method previously discussed and was found to be 210 g/mol. The PEG concentration (wt%) was calculated using the ratio of the aromatic proton integral, $\int H_{BPS-20K}$ to the PEG proton integral, $\int H_{PEG\ 200}$, and it was found to be 59.5 wt% based on the spectrum in Fig. S1-c.

Any molecular structural changes for BPS-20K during extrusion were carefully checked by verifying the sulfonation level (mol%) of BPS, since sulfonated groups are susceptible to thermal degradation. According to Wang et al., $T_{5\%}$ (°C), the temperature for 5% weight loss (by TGA), decreases with increasing sulfonation level [20]. Lee et al. reported thermal desulfonation of BPS polymers at temperatures of 375–420 °C [23]. Although the desulfonation temperature is higher than the potential extrusion temperature, BPS polymer could show a weaker thermal stability in the presence of PEG. To eliminate this possibility, the BPS thermal stability at potential processing temperatures needed to be confirmed. To determine the degree of sulfonation, we used the method reported in the literature with peak assignment as shown in Fig. S1-b [21]. The calculated sulfonation level is 22 mol%, which is similar to the target of 20 mol%, meaning BPS-20K polymer is thermally stable during the extrusion process. Note that as-received BPS-20K polymer shows a sulfonation level of 20–22 mol% by ^{1}H NMR. Based on the ^{1}H NMR analysis, all extruded BPS-20K/PEG 200 blends are thermally stable during extrusion.

To complement the ^{1}H NMR analysis, elemental analysis was also performed. The elemental analysis was used to determine the PEG concentration in the extruded samples, and sulfur (S) was chosen as a reference element because it is only found in the BPS polymer. The S content in the BPS/PEG blends compared to that of the neat BPS polymer is proportional to the BPS concentration in the blends, and, thus, the PEG concentration can be estimated. As shown in Table 6, the calculated PEG concentrations correspond to the target amount of PEG and the results of ^{1}H NMR analysis.

Table 6 summarizes comparisons between the target amount of PEG 200 and the actual amount of PEG 200 in extruded films after compounding and pressing into films. In all cases, the actual amount of PEG 200 corresponds to the target amount of PEG 200, and, thus, PEG 200 loss by evaporation or thermal degradation was insignificant during extrusion. The molecular structure of PEG 200

Table 6
PEG 200 concentration in the extruded BPS-20K/PEG 200 blends after micro-compounding and compression pressing. PEG 200 concentrations were determined by ^{1}H NMR and S (sulfur) elemental analysis.

Intended amount of PEG 200 [wt%]	Processing temperature [°C]	Actual amount of PEG 200 [wt%]		
		^{1}H NMR	S (sulfur) elemental analysis	Average
0	–	0	0	0
20	210	23.3	19.3	21.3
30	200	31.2	33.1	32.2
40	200	42.3	43.0	42.7
50	180	53.8	50.1	52.0
60	160	59.5	62.9	61.2

remains unchanged, and the $\overline{M}_n$ remains near 200 g/mol. The calculated PEG concentrations by the different techniques agree well with each other and confirm that melt processing, within this temperature range, does not lead to thermal degradation or evaporation of the plasticizer.

4. Conclusions

In this work, a disufonated poly(arylene ether sulfone) (BPS) synthesized from the sulfonated monomer combined with a plasticizer, poly(ethylene glycol) (PEG) was used to melt extrude films. PEGs with molecular weights ranging from 200 to 600 g/mol were chosen since they can be conveniently removed by water extraction after membrane extrusion.

BPS and PEG are miscible, and the effect of PEG molecular weight and concentration on the T_g of BPS/PEG blends were investigated. As PEG molecular weight decreases and concentration increases, the blend T_g was depressed significantly. Based on the PEG 200 characterization after isothermal holds at various temperatures and times, these PEGs were found to be thermally stable up to 220 °C for at least 10 min in air or 250 °C for at least 10 min in nitrogen.

Acknowledgments

This work was supported by the NSF Science and Technology Center for Layered Polymeric Systems (Grant 0423914). We acknowledge the generous help from the Department of Chemistry at the University of Texas at Austin for analytical services. Dr. Ben Shoulders provided valuable assistance in the analysis of the ^{1}H NMR data. Ms. Angela Spangenberg and Mr. Steve Sorey helped to perform the ^{1}H NMR measurements. Dr. Sue Mecham from the Department of Chemistry at Virginia Polytechnic Institute and State University helped to measure the molecular weight using SEC.

Appendix A. Supplementary data

Supplementary data related to this article can be found online at http://dx.doi.org/10.1016/j.polymer.2013.11.041

References

[1] Geise GM, Lee H-S, Miller DJ, Freeman BD, McGrath JE, Paul DR. J Polym Sci Part B Polym Phys 2010;48(15):1685–718.
[2] Kucera J. Chem Eng Progr 2008:30–4.
[3] Park HB, Freeman BD, Zhang Z-B, Sankir M, McGrath JE. Angew Chem 2008;47(32):6019–24.
[4] Petersen RJ. J Membr Sci 1993;83(1):81–150.
[5] Xie W, Cook J, Park HB, Freeman BD, Lee CH, McGrath JE. Polymer 2011;52:2244–54.
[6] Xie W, Geise GM, Freeman BD, Lee H-S, Byun G, McGrath JE. J Membr Sci 2012;403–404:152–61.
[7] Xie W, Geise GM, Freeman BD, Lee CH, McGrath JE. Polymer 2012;53:1581–92.
[8] Xie W, Park HB, Lee CH, Byun G, Freeman BD, McGrath JE. Water Sci Technol J Int Assoc Water Pollut Res 2010;61(3):619–24.
[9] Bailey Jr FE, Koleske JV. Properties of poly(ethylene oxide). poly(ethylene oxide). United Kingdom, London: Academic Press, INC. (London) LTD; 1976. pp. 29–31. 136–138.
[10] Chen L, Sheng C-y, Duan Y-x, Zhang J-m. Polymer-Plast Tech Eng 2011;50:412–7.
[11] Ponting M, Hiltner A, Baer E. Macromol Symp 2010;294(1):19–32.
[12] Kim YS, Dong L, Hickner MA, Pivovar BS, McGrath JE. Polymer 2003;44(19):5729–36.
[13] Bebin P, Galiano H. Adv Polym Tech 2006;25(2):127–33.
[14] Bebin P, Galiano H. Adv Polym Tech 2006;25(2):121–6.
[15] Molmeret Y, Chabert F, Kissi NE, Iojoiu C, Mercier R, Sanchez J-Y. Polymers 2011;3:1126–50.
[16] Sanchez J-Y, Chabert F, Iojoiu C, Salomon J, Kissi NE, Piffard Y, et al. Electrochim Acta 2007;53:1584–94.
[17] Molmeret Y, Chabert F, Iojoiu C, Kissi NE, Sanchez J-Y. Extruded proton exchange membranes based on sulfonated polyaromatic polymers for fuel cell applicationIn The XV International Congress on Rheology: the Society of Rheology 80th Annual Meeting, vol. 1027. Monterey, CA: American Institute of Physics; 2008.
[18] Sanchez J-Y, Iojoiu C, Mercier R, Marechal M, Kissi NE, Galiano H, et al. Membrane preparation method comprising the extrusion of a thermoplastic polymer bearing alkaline groupings, United States Patent no. 7,973,089 B2; 2011.
[19] Sanchez J-Y, Iojoiu C, Piffard Y, Kissi NE, and Chabert F. Extrusion of a thermoplastic polymer bearing acid ionic groupings, United States Patent no. 7956095 B2; 2011.
[20] Wang F, Hickner M, Kim YS, Zawodzinski TA, McGrath JE. J Membr Sci 2002;197:231–42.
[21] Li Y, Wang F, Yang J, Liu D, Roy A, Case S, et al. Polymer 2006;47:4210–7.
[22] Lodge TP, Wood ER, Haley JC. J Polym Sci Part B Polym Phys 2005;44(4):756–63.
[23] Lee CH, VanHouten D, Lane O, McGrath JE, Hou J, Madsen LA, et al. Chem Mater 2011;23(4):1039–49.
[24] Sigma-Aldrich. Poly(ethylene glycol) average Mn 300 (cat# 202371) http://www.sigmaaldrich.com/catalog/product/aldrich/202371?lang=en&region=US; 2012.
[25] Sigma-Aldrich. Poly(ethylene glycol) average Mn 400 (cat# 202398) http://www.sigmaaldrich.com/catalog/product/aldrich/202398?lang=en&region=US; 2012.
[26] Sigma-Aldrich. In: Sigma-Aldrich, editor. Poly(ethylene glycol) 600 (cat# 87333). http://www.sigmaaldrich.com/catalog/product/sigma/87333?lang=en&region=US; 2012.
[27] Sigma-Aldrich. Poly(ethylene glycol) average mol wt 200 (cat# P3015) http://www.sigmaaldrich.com/catalog/product/sial/p3015?lang=en&region=US; 2012.
[28] Faucher JA, Koleske JV, Santee ER, Stratta JJ, Wilson CW. J Appl Phys 1966;37(11):3962–4.
[29] Gaikwad AN, Wood ER, Ngai T, Lodge TP. Macromolecules 2008;41:2502–8.
[30] Bigger SW, Delatycki JS, Billingham NC. Polym Int 1991;26:181–6.
[31] Hiemenz PC, Lodge TP. Glass transition. Polymer chemistry. CPC Press; 2007. p. 494.
[32] Fox TG, Loshaek S. J Polym Sci 1955;15:371–90.
[33] Fox TG, Flory PJ. J Appl Phys 1950;21:581–91.
[34] Connor TM, Read BE, Williams G. J Appl Chem 1964;14:74–80.
[35] Foreman J, Sauerbrunn SR, and Marcozzi CL. Exploring the sensitivity of thermal analysis techniques to the glass transition: TA Instruments Inc.
[36] Kalika DS. Viscoelastic characterization of polymer blends. In: Paul DR, Bucknall CB, editors. Polymer blends formulation, vol 1. Canada: John Wiley & Sons, Inc; 2000. pp. 291–317.
[37] Cowie JMG, Arrighi V. Miscibility and relaxation processes in blends. In: Shonaike GO, Simon GP, editors. Polymer blends and alloys. New York, USA: Marcel Dekker, Inc.; 1999. pp. 81–124.
[38] Hofmann GH. Polymer blend modification of PVC. In: Walsh DJ, Higgins JS, editors. Polymer blends and mixtures. The Netherlands: Martinus Nijhoff Publishers; 1985. pp. 117–48.
[39] Dionisio M, Fernandes AC, Mano JF, Correia NT, Sousa RC. Macromolecules 2000;33:1002–11.
[40] Pielichowski K, Flejtuch K. Polym Advan Technol 2002;13:690–6.
[41] Ghious N, Benaniba MT. Int J Polym Mater 2010;59:463–74.
[42] Wilson AS. Plasticizers: principles and practice. Cambridge, UK: The Institute of Materials; 1995.
[43] Eisenberg A, Kim JS. Plasticization. Introduction to ionomers. Canada: John Wiley & Sons, Inc; 1998. pp. 244–56.
[44] Nielsen LE, Buchdahl R, Levreault R. J Appl Phys 1950;21:607–15.
[45] Schmeieder K, Wolf K. Kolloid-Zeitschrift 1952;127:65–78.
[46] Nakamura K. J Polym Sci: Polym Phys Ed 1975;13:137–49.
[47] Huang H-H, Yorkgitis EM. J Macromol Sci, Phys 1993;B32(2):163–81.
[48] Curtis AJ. Dielectric properties of polymeric systems. In: Birks JB, Schulman JH, editors. Progress in dielectrics, vol. 2. Hertfordshire, UK: Heywood & Company Ltd.; 1960. pp. 31–76.
[49] McGrum NG, Read BE, Williams G. Anelastic and dielectric effects in polymeric solids. UK: John Wiley & Sons Ltd; 1947.

[50] Read BE. Polymer 1962;3:529–42.
[51] Craig DQM. Thermochim Acta 1995;248:189–203.
[52] Ceccorulli G, Pizzoli M, Scandola M, Alfonso GC, Turturro A. Polymer 1989;30(7):1251–6.
[53] Allen G, McAinsh J, Jeffs GM. Polymer 1971;12(2):85–100.
[54] Han S, Kim C, Kwon D. Polymer 1997;38(2):317–23.
[55] Mortensen MN, Egssaard H, Hvilsted S, Shashoua Y, Glastrup J. J Archaeol Sci 2012;39:3341–8.
[56] Knop K, Hoogenboom R, Fischer D, Schuber U. Angew Chem Int Ed 2010;49:6288–308.
[57] Pielichowski K, Flejtuch K. J Anal Appl Pyrol 2005;73:131–8.
[58] Glastrup J. Polym Degrad Stab 1996;52:217–22.
[59] Malik P, Castro M, Carrot C. Polym Degrad Stab 2006;91:634–40.
[60] Kitahara Y, Takahashi S, Fujii T. Chemosphere 2012;88:663–9.
[61] Mkhatresh OA, Heatley F. Polym Int 2004;53:1336–42.
[62] Mkhatresh OA, Heatley F. Macromol Chem Phys 2002;203:2273–80.
[63] Yang L, Heatley F, Blease TG, Thompson RIG. Eur Polym J 1996;32(5):535–47.
[64] Silverstein RM, Webster FX, Kiemle D. Spectrometric identification of organic compounds. 7th ed. John Wiley & Sons Inc; 2005.
[65] Scheris J, Bigger SW, Delatycki O. Polymer 1991;32(11):2014–9.
[66] Lin H, Kai T, Freeman BD, kalakkunnath S, Kalika D. Macromolecules 2005;38:8381–93.